Annals of Science and Inquiry
Vol. 2 No. 11 (2026)

The Same Net Battery Withdrawal Conceals Different Charge Throughput

Donna Howard · Isabella Hart · Michael J. Anderson

Published: November 26, 2026 | Article 1192

Abstract

Equal net discharge specifies the difference between outgoing and incoming charge. It does not specify how much charge crossed the measurement boundary in total. I integrated the signed current in 27 laboratory drive records and matched each observation window from the first 1 Ah of net discharge to the first 3 Ah. The resulting median gross throughput was 3.319 Ah for BCDC, 2.525 Ah for US06 and 2.191 Ah for HWFET, although every window represented exactly 2 Ah of net withdrawal under the integration rule. The order held in all nine matched cell-and-temperature comparisons and under two shifted windows. Recording only the net change omitted 39.7% of gross throughput in the median BCDC record and 8.7% in the median HWFET record. The choice of accounting variable materially changes how these measured profiles are compared.

The Same Net Battery Withdrawal Conceals Different Charge Throughput

Abstract

Equal net discharge specifies the difference between outgoing and incoming charge. It does not specify how much charge crossed the measurement boundary in total. I integrated the signed current in 27 laboratory drive records and matched each observation window from the first 1 Ah of net discharge to the first 3 Ah. The resulting median gross throughput was 3.319 Ah for BCDC, 2.525 Ah for US06 and 2.191 Ah for HWFET, although every window represented exactly 2 Ah of net withdrawal under the integration rule. The order held in all nine matched cell-and-temperature comparisons and under two shifted windows. Recording only the net change omitted 39.7% of gross throughput in the median BCDC record and 8.7% in the median HWFET record. The choice of accounting variable materially changes how these measured profiles are compared.

A net charge change leaves the path open

Battery state is often communicated as a level or change in level. Over a dynamic test, the net amount of charge withdrawn is an intuitive result because it indicates how much more charge left the electrical terminals than entered them over the interval. A current trace also contains the two directional quantities needed to calculate that balance. Saving the balance alone removes this information. A test with several inputs of charge can arrive at a net withdrawal of 2 Ah after a larger total outward charge, while a test with little return can reach the same amount with less outward flow. The net outcome does not tell us how much electrical passage the cell experienced along the way.

Xu et al. (2026) study joint estimation of state of charge, state of health and power capacity with a common treatment of safety boundaries. The task of joint estimation makes choice of history variables consequential because a quantity that tracks change of charge well can omit some of the history used to characterize cycling exposure. Zhang et al. (2021) similarly specify several estimated battery states in one architecture. Individual quantities may use different inputs and time horizons, as illustrated by the state-of-power formulations of Lai et al. (2024) and Zou et al. (2018). The present study evaluates the measured charge history alone. It asks how much bidirectional movement can lie behind the same net withdrawal in otherwise comparable recorded tests.

The distinction is visible in prior work at both vehicle and cell scales. Björnsson and Karlsson (2016) examined the dependence of recoverable braking energy on observed driving patterns and drivetrain assumptions. Szumska and Jurecki (2022) compare regeneration across vehicle operating conditions, while Xie et al. (2020) trace energy and range consequences of differing traffic and driving conditions with a vehicle model. Kim et al. (2026) develop stochastic operating profiles for use in battery degradation experiments. These studies show that the timing and direction of loading in a drive are substantive features. They also illustrate why a cell's measured inward ampere-hours are a different outcome from recoverable vehicle braking energy. The electrical terminal measurement records charge crossing that boundary. Neither vehicle speed nor mechanical braking effort is needed to compute the cell-level question studied here.

The research question is how much gross charge throughput varies between repeatedly applied drive profiles when state excursion is matched by absolute net ampere-hours withdrawn. The design compares three programmed laboratory profiles in each of nine matched cell-and-chamber combinations. Instead of ranking traces by their final signed totals, it asks what a record limited to that signed change would omit.

The comparison is a descriptive accounting exercise on observed current. A measured difference in gross throughput is separable from an inference about capacity or lifetime.

The same amount left the cell in every comparison window

The experimental source is a TU Berlin release of drive-cycle measurements from three LG INR21700 M50LT cells (Yao et al., 2026b), with experimental setup and state-estimation context described by Yao et al. (2026a). I used 27 of the archive's split drive files. The three measured profiles are Braunschweig City Driving Cycle (BCDC), US06 and Highway Fuel Economy Test (HWFET). Each is represented for each cell and chamber setpoint of 5, 25 and 45 °C. Each split file contains the profile applied repeatedly to a prescribed endpoint. These records are laboratory replays of current-bearing profiles on individual cells, rather than single trips made by instrumented vehicles. Only the recorded elapsed-time and current columns were read. No archive state-of-charge estimates, voltage channels or temperature values were inputs to the integration. The setpoint remains an experimental grouping variable.

Discharge appears as negative current in these records. After reversing the sign to work in the direction of charge withdrawal, I calculate the net withdrawal from the start of each split time series. The primary window begins at the first attainment of 1 Ah of net withdrawal and ends at the first attainment of 3 Ah of net withdrawal. Every retained file reaches both levels. A window is defined by measured signed accumulation within the file. It does not require a nominal cell capacity, assume an exactly measured starting state of charge or use the source's state-of-charge normalization. The archive notes that parts of commanded regeneration near the beginning of the profile have been clipped. Starting at 1 Ah of measured net withdrawal limits the focus to a later operated section, while the results remain conditional on the complete published drive procedure including any clipping.

I integrated current over original elapsed-time intervals using a linear interpolant for each adjacent pair of observed values. With a current sign reversal inside one interval, splitting the interpolant at zero gives separate contributions to charge out of and into the cell. Linear current implies a quadratic cumulative integral inside an interval. I located the first crossings to this integrated curve and accounted for only the part of each boundary interval inside the window. This procedure preserves the sign changes rather than applying a magnitude to an interval average after the currents in opposite directions have cancelled. The recorded files contain 3,724,236 time-current rows, and 1,666,460 observed time stamps occupy the primary windows. The largest interval between neighboring recorded times was 0.2 seconds. More precise computed crossing values describe the interpolation model and do not improve the underlying instrument's precision. Coulomb-counting work by Ng et al. (2009) and Lee and Won (2023) addresses how current integration and efficiency information enter state estimation. The calculation here deliberately uses raw terminal ampere-hours, without an efficiency factor, because those are the electrical transfers being compared.

For each window I recorded outward ampere-hours, returned ampere-hours, their sum and elapsed duration. Let D and R denote the two nonnegative directional quantities. Net withdrawal is D minus R and gross charge throughput is D plus R. With net withdrawal fixed at 2 Ah, gross exceeds net by twice the returned amount. A natural comparison is thus the share of gross movement that would disappear in a record containing only net charge. Counting the return once would miss the extra outward movement that also has to occur to end at the same amount withdrawn. This arithmetic relationship specifies what to measure and helps interpret the contrast. It does not establish the size of the empirical gaps, which depend on how much inward current the individual profiles actually produced.

I report the median and observed range across the nine records per profile and compare profiles within the same cell and setpoint. Matching is valuable here because otherwise observations from different

temperatures and cells could constitute the apparent profile contrast. Bland and Altman (2007) discuss the reasoning for retaining paired comparisons between measurements, and Hyndman and Fan (1996) discuss the sample-quantile conventions that affect summaries of small measured groups. I use paired medians and ranges with no confidence claims about a population from three cells. Two sensitivity checks shift both boundaries, to 0.5–2.5 Ah and 1.5–3.5 Ah. They retain the same net change but inspect different spans of the recorded paths.

A longer and more bidirectional path at equal withdrawal

All 27 calculated primary windows represented 2 Ah of net withdrawal to within numerical integration error. The profiles separated clearly once both directions were counted. Median gross charge was 3.319 Ah for BCDC, 2.525 Ah for US06 and 2.191 Ah for HWFET. Outward charge alone was also greater in BCDC, with a median 2.659 Ah compared with 2.263 Ah and 2.095 Ah in the other two profiles. The corresponding inward charge was 0.659, 0.263 and 0.095 Ah. Those amounts quantify what the electrical records show inside the matched windows. In the BCDC record with median throughput, discarding the direction history would miss roughly two fifths of the gross ampere-hours. In the median HWFET record, it would miss less than one tenth.

Table 1. *Directional charge movement and duration between first attainment of 1 and 3 Ah net withdrawal. Each row uses nine records. Charge and time entries are medians except for the observed gross range. The omitted share is the difference between gross and net divided by gross.*

Drive profile	Records	Net (Ah)	Outward (Ah)	Returned (Ah)	Gross (Ah)	Gross range (Ah)	Gross omitted by net alone	Time (min)
BCDC	9	2.000	2.659	0.659	3.319	3.299–3.328	39.7%	169.13
US06	9	2.000	2.263	0.263	2.525	2.495–2.536	20.8%	94.55
HWFET	9	2.000	2.095	0.095	2.191	2.190–2.199	8.7%	46.38

The ordering was the same in each matched cell and setpoint. The median BCDC-minus-HWFET excess was 1.128 Ah across the nine paired contrasts, with a range of 1.100–1.137 Ah. The median US06-minus-HWFET excess was 0.334 Ah, with a range of 0.296–0.346 Ah. BCDC exceeded US06 by 0.793 Ah at the median. The observed file ranges in Table 1 did not overlap between profiles. These results describe how the same tests separated within a particular archive. The matched pairs are useful as a check that the ranking is present at all conditions sampled here, without counting the nine pairs as independent experiments on different battery designs.

Elapsed time put those differences in context. Median times were 169.13, 94.55 and 46.38 minutes for BCDC, US06 and HWFET respectively. The equal net change fixes the charge outcome in the same way for all records. It does not equalize time under the varying load, nor does it impose the same current path along the way. Figure 1 shows the returned charge and its matching extra outward component on top of the common 2 Ah base. The points in the right panel show that both time and gross movement differed among the observed profiles. Their association in these three prescribed drives should not be interpreted as an effect of time on cumulative inward current under other conditions.

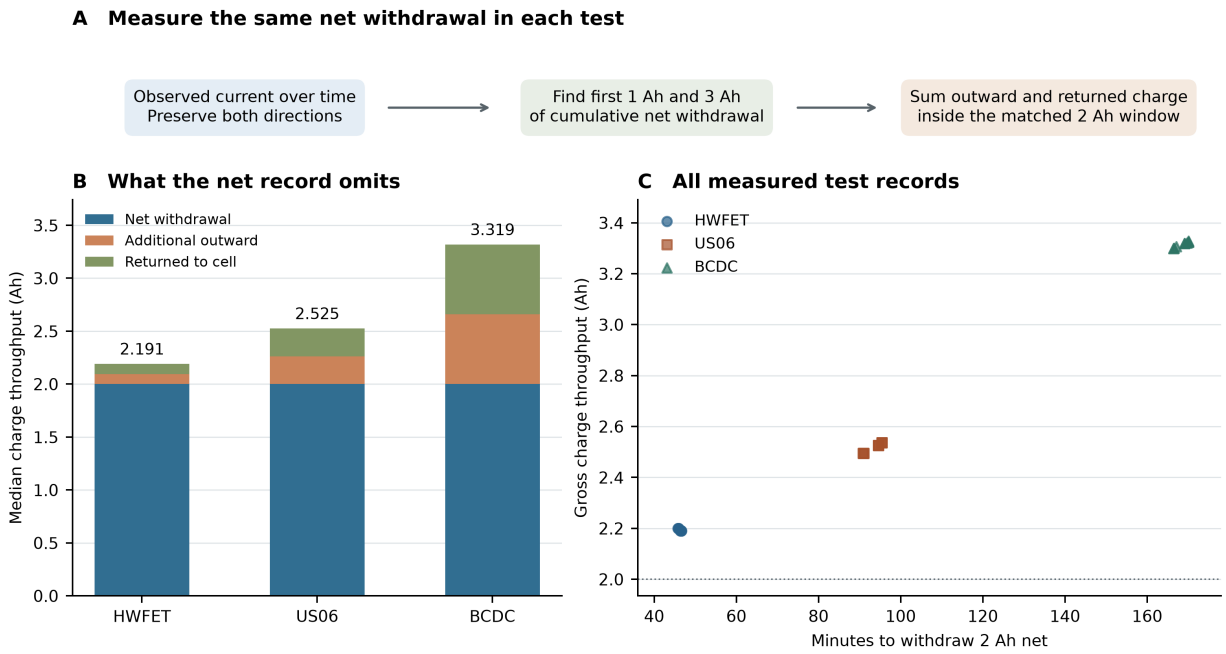


Figure 1. A specifies the matching and integration rule. B partitions median gross throughput into the 2 Ah net withdrawal and the two directional quantities that cancel in the net record. C plots each measured profile window by its observed duration and integrated gross charge. Repeated settings may generate overlapping plot symbols.

The same ranking held in the shifted windows. At 0.5–2.5 Ah the profile medians were 3.253 Ah for BCDC, 2.483 Ah for US06 and 2.186 Ah for HWFET. At 1.5–3.5 Ah those values were 3.329, 2.504 and 2.194 Ah. Every pairwise ordering remained positive in its previous direction in all nine matched cell-and-setting comparisons for both alternative windows. In particular, the median paired BCDC-minus-HWFET excess varied from 1.068 to 1.134 Ah across the candidate windows. Selecting a particular band changes some of the numerical contrasts because it changes which observed episodes are included. It did not remove the separation in this archive.

Interpreting throughput without treating it as cell wear

These findings concern terminal charge, which is an input to certain accounts of battery use. Persistent aging can be monitored through a measured performance outcome, as in work on degradation diagnostics by Birkl et al. (2017) or early-life cycle prediction by Severson et al. (2019). Models such as those of Schmalstieg et al. (2014) and Horstkötter et al. (2023) represent the influence of distinct operating histories on capacity. Direct comparative data also show different degradation patterns across conditions, as studied by Preger et al. (2020) and Kirkaldy et al. (2024), and a profile-dependent distinction between dynamic and constant cycling, as found by Geslin et al. (2025). Those results depend on experimental contrasts that include actual degradation outcomes. Here there is no corresponding longitudinal observation with which to rank these profiles by their wear.

The same distinction matters for claims about bidirectional operation. Keil and Jossen (2015) and Keil and Jossen (2017) tested regenerative driving loads with different associations to aging in their parameter spaces and timescales. Peterson et al. (2010) compare realistic vehicle and vehicle-to-grid battery use. Uddin et al. (2017) incorporate multiple aging inputs in evaluating a bidirectional use case. The present evidence simply gives the magnitude that disappears when a current history is stored as a net balance. It should not be interpreted as if an inward charge that cancels in the net record necessarily creates the same aging as the outward charge that it offsets. Even a model that uses measured throughput would still have to choose how to treat charge direction, intervening rest, history and elapsed time.

The observed gap can also clarify requirements for recordkeeping. Plett (2004) illustrates how a state estimator may retain histories through an evolving model state. An archive reduced to its net endpoints cannot reconstruct the pair of directional contributions without further assumptions about the underlying paths. Saving separate totals preserves gross movement, but it still loses the time order of the inward and outward events. A time-resolved model or a study of current reversals would need the chronological samples. This hierarchy of coarse and detailed data can guide what quantity to retain for a stated analytical purpose, even if the final report only compares windows at equal net withdrawal.

The archive contains three cells of one design at laboratory chamber settings and the three chosen profile families. It cannot establish typical annual throughput on the road or quantify relative recovery efficiency at the drivetrain. The contrast is in ampere-hours at the cell terminals, so the record lacks the voltage, power and mechanical measurements used for energy-based interpretation here. The estimates are conditional on each profile's test implementation and on absolute withdrawal bands rather than a fixed percentage of usable capacity. A future comparison using the same labels at a different cell scale or where charging-current constraints differ would need its own retained current path and its own checks on matching. None of those extensions changes the calculation for these measured paths.

Conclusion

Matching the drives at a net 2 Ah withdrawn made their net records identical while leaving a 1.128 Ah median matched difference in gross movement between BCDC and HWFET. The two shifted bands and all nine paired settings preserved the ranking. Reporting both separately integrated directions gives a concrete description of the charge moved along the measured current path, without drawing conclusions about the cells' later state of health.

Data and code availability

The source archive identifiers and selected file hashes are linked in the provenance record, which also gives the exact comparison bands and replay instructions. dos Reis et al. (2021) discuss why archiving protocol and measurement details matters for battery-data reuse. The traceable source identification and explicit accounting choices follow provenance and documentation principles emphasized by Wilkinson et al. (2016) and Gebru et al. (2021). The analysis exposes the calculation from current and time through to the table, consistent with Peng (2011) on computational reproducibility. No independent measurements outside the deposited records enter the reported comparisons.

References

Birkl, Christoph R.; Roberts, Matthew R.; McTurk, Euan; Bruce, Peter G.; Howey, David A. (2017). Degradation diagnostics for lithium ion cells. *Journal of Power Sources, 341, 373–386*. DOI.

Björnsson, Lars-Henrik; Karlsson, Sten (2016). The potential for brake energy regeneration under Swedish conditions. *Applied Energy, 168, 75–84*. DOI.

Bland, J. Martin; Altman, Douglas G. (2007). Agreement Between Methods of Measurement with Multiple Observations Per Individual. *Journal of Biopharmaceutical Statistics, 17(4), 571–582*. DOI.

dos Reis, Gonçalo; Strange, Calum; Yadav, Mohit; Li, Shawn (2021). Lithium-ion battery data and where to find it. *Energy and AI, 5, 100081*. DOI.

Gebru, Timnit; Morgenstern, Jamie; Vecchione, Briana; Vaughan, Jennifer Wortman; Wallach, Hanna; III, Hal Daumé; Crawford, Kate (2021). Datasheets for datasets. *Communications of the ACM, 64(12), 86–92*. DOI.

Xu, Dan; Chen, Huangyin; Gui, Hao (2026). Unified Online Estimation Method for SOC, SOH, and Power Capacity Considering Safety Boundary Consistency in Battery Management Systems. *2026 International Conference on Electrical, Control and Information Technology (ECITech), 133–137*. DOI.

Geslin, Alexis; Xu, Le; Ganapathi, Devi; Moy, Kevin; Chueh, William C.; Onori, Simona (2025). Dynamic cycling enhances battery lifetime. *Nature Energy, 10(2), 172–180*. DOI.

Horstkötter, Ivo; Bäker, Bernard (2023). An application-oriented lithium-ion battery degradation modelling framework for ageing prediction. *Journal of Energy Storage, 60, 106640*. DOI.

Hyndman, Rob J.; Fan, Yanan (1996). Sample Quantiles in Statistical Packages. *The American Statistician, 50(4), 361–365*. DOI.

Keil, Peter; Jossen, Andreas (2015). Aging of Lithium-Ion Batteries in Electric Vehicles: Impact of Regenerative Braking. *World Electric Vehicle Journal, 7(1), 41–51*. DOI.

Keil, Peter; Jossen, Andreas (2017). Impact of Dynamic Driving Loads and Regenerative Braking on the Aging of Lithium-Ion Batteries in Electric Vehicles. *Journal of The Electrochemical Society, 164(13), A3081–A3092*. DOI.

Kim, Sehwan; Jeong, Jinho; Jin, Jaemin; Jung, Insoo; Oh, Ki-Yong (2026). Stochastic Operational Driving Cycles of an Electric Vehicle Battery System for Degradation Experiments. *International Journal of Energy Research, 2026(1), 9134230*. DOI.

Kirkaldy, Niall; Samieian, Mohammad A.; Offer, Gregory J.; Marinescu, Monica; Patel, Yatish (2024). Lithium-ion battery degradation: Comprehensive cycle ageing data and analysis for commercial 21700 cells. *Journal of Power Sources, 603, 234185*. DOI.

Lai, Xin; Yuan, Ming; Tang, Xiaopeng; Zheng, Yuejiu; Zhu, Jiajun; Sun, Yuedong; Zhou, Yuanqiang; Gao, Furong (2024). State-of-power estimation for lithium-ion batteries based on a frequency-dependent integer-order model. *Journal of Power Sources, 594, 234000*. DOI.

Lee, Jeong; Won, Jehyuk (2023). Enhanced Coulomb Counting Method for SoC and SoH Estimation Based on Coulombic Efficiency. *IEEE Access, 11, 15449–15459*. DOI.

Ng, Kong Soon; Moo, Chin-Sien; Chen, Yi-Ping; Hsieh, Yao-Ching (2009). Enhanced coulomb counting method for estimating state-of-charge and state-of-health of lithium-ion batteries. *Applied Energy, 86(9), 1506–1511*. DOI.

Peng, Roger D. (2011). Reproducible Research in Computational Science. *Science, 334(6060), 1226–1227*. DOI.

Peterson, Scott B.; Apt, Jay; Whitacre, J.F. (2010). Lithium-ion battery cell degradation resulting from realistic vehicle and vehicle-to-grid utilization. *Journal of Power Sources, 195(8), 2385–2392*. DOI.

Plett, Gregory L. (2004). Extended Kalman filtering for battery management systems of LiPB-based HEV battery packs. *Journal of Power Sources, 134(2), 252–261*. DOI.

Preger, Yuliya; Barkholtz, Heather M.; Fresquez, Armando; Campbell, Daniel L.; Juba, Benjamin W.; Romàn-Kustas, Jessica; Ferreira, Summer R.; Chalamala, Babu (2020). Degradation of Commercial Lithium-Ion Cells as a Function of Chemistry and Cycling Conditions. *Journal of The Electrochemical Society, 167(12), 120532*. DOI.

Schmalstieg, Johannes; Käbitz, Stefan; Ecker, Madeleine; Sauer, Dirk Uwe (2014). A holistic aging model for Li(NiMnCo)O2 based 18650 lithium-ion batteries. *Journal of Power Sources, 257, 325–334*. DOI.

Severson, Kristen A.; Attia, Peter M.; Jin, Norman; Perkins, Nicholas; Jiang, Benben; Yang, Zi; Chen, Michael H.; Aykol, Muratahan; Herring, Patrick K.; Fraggedakis, Dimitrios; Bazant, Martin Z.; Harris, Stephen J.; Chueh, William C.; Braatz, Richard D. (2019). Data-driven prediction of battery cycle life before capacity degradation. *Nature Energy, 4(5), 383–391*. DOI.

Szumska, Emilia M.; Jurecki, Rafał (2022). The Analysis of Energy Recovered during the Braking of an Electric Vehicle in Different Driving Conditions. *Energies, 15(24), 9369*. DOI.

Uddin, Kotub; Jackson, Tim; Widanage, Widanalage D.; Chouchelamane, Gael; Jennings, Paul A.; Marco, James (2017). On the possibility of extending the lifetime of lithium-ion batteries through optimal V2G facilitated by an integrated vehicle and smart-grid system. *Energy, 133, 710–722*. DOI.

Wilkinson, Mark D.; Dumontier, Michel; Aalbersberg, IJsbrand Jan; Appleton, Gabrielle; Axton, Myles; Baak, Arie; Blomberg, Niklas; Boiten, Jan-Willem; da Silva Santos, Luiz Bonino; Bourne, Philip E.; Bouwman, Jildau; Brookes, Anthony J.; Clark, Tim; Crosas, Mercè; Dillo, Ingrid; Dumon, Olivier; Edmunds, Scott; Evelo, Chris T.; Finkers, Richard; Gonzalez-Beltran, Alejandra; Gray, Alasdair J.G.; Groth, Paul; Goble, Carole; Grethe, Jeffrey S.; Heringa, Jaap; 't Hoen, Peter A.C; Hooft, Rob; Kuhn, Tobias; Kok, Ruben; Kok, Joost; Lusher, Scott J.; Martone, Maryann E.; Mons, Albert; Packer, Abel L.; Persson, Bengt; Rocca-Serra, Philippe; Roos, Marco; van Schaik, Rene; Sansone, Susanna-Assunta; Schultes, Erik; Sengstag, Thierry; Slater, Ted; Strawn, George; Swertz, Morris A.; Thompson, Mark; van der Lei, Johan; van Mulligen, Erik; Velterop, Jan; Waagmeester, Andra; Wittenburg, Peter; Wolstencroft, Katherine; Zhao, Jun; Mons, Barend (2016). The FAIR Guiding Principles for scientific data management and stewardship. *Scientific Data, 3(1), 160018*. DOI.

Xie, Yunkun; Li, Yangyang; Zhao, Zhichao; Dong, Hao; Wang, Shuqian; Liu, Jingping; Guan, Jinhuan; Duan, Xiongbo (2020). Microsimulation of electric vehicle energy consumption and driving range. *Applied Energy, 267, 115081*. DOI.

Yao, Jiaqi; Droese, Dominik; Kowal, Julia (2026a). Joint online estimation of state of charge and internal temperature of lithium-ion batteries with multi-task learning. *Journal of Energy Storage, 155, 121468*. DOI.

Yao, Jiaqi; Droese, Dominik; Kowal, Julia (2026b). Lithium-Ion Battery Internal Temperature Dataset. *Technische Universität Berlin, DepositOnce*. DOI.

Zhang, Tao; Guo, Ningyuan; Sun, Xiaoxia; Fan, Jie; Yang, Naifeng; Song, Junjie; Zou, Yuan (2021). A Systematic Framework for State of Charge, State of Health and State of Power Co-Estimation of Lithium-Ion Battery in Electric Vehicles. *Sustainability, 13(9), 5166*. DOI.

Zou, Changfu; Klintberg, Anton; Wei, Zhongbao; Fridholm, Björn; Wik, Torsten; Egardt, Bo (2018). Power capability prediction for lithium-ion batteries using economic nonlinear model predictive control. *Journal of Power Sources, 396, 580–589*. DOI.